Sensors & Diagnostics

PAPER

View Article Online
View Journal | View Issue

Cite this: *Sens. Diagn.*, 2023, **2**, 337

Design and development of a fluorometric and colorimetric sensor for toxic cyanide detection by pyridinium scaffolds: live cell imaging and real sample analysis†

Kannan Jamuna,[a] Santhalingam Gayathri,[b] Shanmugam Sivakumar *[a] and Balasubramaniem Ashokkumar [b]

Received 12th September 2022,
Accepted 18th November 2022

DOI: 10.1039/d2sd00163b

rsc.li/sensors

Polyheteroaryl pyridinium-based indenophenanthridine is synthesized using the conventional method. The synthesized pyridinium core indenophenanthridine detects cyanide ion (CN^-) in a ratiometric manner with an excellent detection limit (1.2 nM). The CN^- sensing ability of the probe was treated for practical applications in food extracts, water samples, and U87 cell lines. The probe successfully detected the CN^- anion in real samples and cell lines.

Organic fluorophore featured with donor–acceptor (D–A) frameworks shows immerse applications in OLEDs, solar cells, laser dyes, biosensors, cell imaging, chemosensors, *etc.*[1] In particular, tuning and controlling the optical properties of this material demonstrating practical applications in acid and metal sensors, monitoring the pH effect on the biological system, and display devices[2] have been reported. Phenanthridine systems have significant optical properties owing to the donor–acceptor (D–A) backbone.[3] Most importantly, the aromatic amine group is responsible for tuning the optical properties by perturbing the D–A nature of the fluorophore.[4] The alkalinity of the pyridine ring is the binding site for various stimuli responses, such as intramolecular hydrogen bonding[5] and interaction with multiple metal cations.

Anions play a crucial role in biological functions, industrial processes, medicine, *etc.* CN^- anions are highly toxic elements[6,7] that have many harmful effects on human physiological conditions when exposed.[8] In living cells, cyanide anions are readily bound with the heme unit Fe^{3+} and block the oxygen supply and cellular respiration.[9,10] The WHO has recommended the allowed level of cyanide ions in drinking water (below <1.9 μM);[11] however, despite their toxic nature, CN^- anions are widely used in industrial and pharmacological applications; these industrial wastes pollute water, which causes dangerous effects on human health.[12–16] Moreover, many cyanogenic plants, such as cassava, almond nuts, and sprouted potatoes, can release poisonous hydrogen cyanide when hydrolyzed.[17–20] Daily consumption of cyanide anion in the human body causes serious effects, such as permanent nervous problems, mental confusion, and death.[21–23] Based on its toxic nature, it is highly desirable to develop a CN^- anion sensor that is simple, highly selective, cost-effective, and has a low-level detection limit.[24] Recently, cyanide ions have attracted much attention from chemosensors because of their unique reactivity towards various organic functional groups, such as C=O,[25] C=C,[26] and C=N;[27] additionally, these approaches create strong chemical bonds and give irreversible formation using a sensing process called chemodosimeters.[25] Various wide ranged chemical motifs are used for the detection of cyanide concentration in a reaction-based manner, such as acridinium salts,[26] benzyl derivatives,[27] dicyanovinyl derivatives,[28] squaraine,[29] and trifluoroacetophenone derivatives.[30] Recently, triazolopyridinium salt has been used for sensing cyanide ions through the ring opening method.[31] However, they have some limitations, such as complex synthetic routes, a lower limit of detection, a high analyte concentration requirement, and poor application in live cells. The development of sensors for cyanide with a good limit of detection, low quantity of analyte, and excellent live cell applications is highly needed.

The D–A-based indenophenanthridine has been reported for selectively sensing of Fe^{3+} metal ion owing to its free nitrogen atom.[32] When pyridine becomes pyridinium moiety, the α carbon gets an effective nucleophilic center, making a probe eligible for sensing towards anionic species. On this

[a] *Department of Organic Chemistry, School of Chemistry, Madurai Kamaraj University, Madurai-625021, India. E-mail: shivazzen@mkuniversity.org*
[b] *School of Biotechnology, Madurai Kamaraj University, Madurai-625021, India*
† Electronic supplementary information (ESI) available. See DOI: https://doi.org/10.1039/d2sd00163b

basis, we synthesized a pyridinium quaternary ammonium complex (Me-INDP). The synthesized probe Me-INDP selectively senses the CN^- anion *via* a nucleophilic reaction mechanism with an excellent limit of detection without ring opening.

Results and discussion

Synthetic route

Probe INDP was synthesized *via* the [4 + 2] annulation following our previous work (already mentioned in reference on page 2), and a one-step reaction involved the synthesis of probe Me-INDP. The quaternary ammonium complex Me-INDP was prepared using synthesized indenophenanthridine (INDP) treated with methyl iodide (MeI) at cold conditions (0 °C) in DCM at nitrogen atmospheric for 12 hours, as shown in Scheme 1. This simple synthetic route significantly enhanced the yield of the product, purity, and cost-effectiveness. The structure of the probe Me-INDP is fully characterized by ^{1}H NMR, ^{13}C NMR, and mass spectrometry.

Optical responses towards CN^- anion. The colorimetric and fluorometric behavior of the probe Me-INDPs with cyanide anion was investigated in the ACN/H_2O (9 : 1) ratio. The probe Me-INDP (10 μL) showed an intense emitting peak at 580 nm (Fig. S1†). The UV-vis spectrum of Me-INDP showed three peaks at 320, 370, and 420 nm, which were assigned to n–π*, π–π* transitions (Fig. S3†). With the addition of cyanide ions, the optical density (OD) values of the three peaks gradually decreased and were constant when the cyanide ion concentration reached 10 μL (Fig. 1a). With the addition of cyanide, the initial emitting peak at 580 nm gradually decreased and formed a new peak at 480 nm. A large blue shift at 100 nm was obtained when the cyanide anion reacted with the probe Me-INDP; simultaneously, the isometric point at 500 nm in the sigmoidal graph (Fig. S2†) showed that Me-INDP was sensitive toward CN^- in a radiometric manner. A well isosbestic point indicates that a chemical process occurs between two reactive species and confirms the formation of a new fluorophore with a cyanine adduct. The conversion of the quaternary ammonium complex to the pyridine moiety of Me-IND by the addition of CN^- ion was the reason for obtaining the blue shift. Initially, internal charge transfer (ICT) occurs between the acceptor system (+N–Me group) and aromatic donor groups; when CN^- is attached, the N–Me becomes the donor, and the strong electron withdrawing CN^- on the attached aromatic system becomes the acceptor. Thus, the changes in the ICT mechanism and loss of conjugation were the reasons for obtaining the blue shift. With the continuous addition of cyanide ion (10 μL) into the probe solution, the intensity of the emitted peak at 580 nm was quenched completely and reached a maximum of 480 nm (Fig. 1b).

Further, no changes were observed during the excess addition of cyanide ions to the solution. In the absence of cyanide ion, the fluorescence intensity ratio (I_{480}/I_{580}) of Me-INDP was calculated (0.17). The value increased when cyanide ion was added and reached a constant at 10 μL. The (I_{480}/I_{580}) ratio shows good linearity with a cyanide concentration of 0–10 μL (Fig. S4†). The binding constant [Ks] between probe Me-INDP and cyanide was calculated as 3.1×10^7 M^{-1} using the Stern–Volmer plot (Fig. 2). The LOD value was calculated from $3\sigma/S$, and the obtained value is 1.2×10^{-9} M. It was below the level of the approved cyanide concentration in drinking water by the World Health Organization (WHO) (<1.9 μM). To the best of our knowledge, this simple methylated pyridinium salt acts as a chemodosimeter with a low requirement for analyte, excellent LOD, and high binding affinity compared with those in the literature (Table 1).

To evaluate the selectivity of Me-INDP, various anions (10 μL), such as F^-, Cl^-, Br^-, I^-, OAc^- PO_4^{2-}, NO_2^{2-}, SCN^-, CO_3^{2-}, and SO_4^{2-}, are investigated in an ACN/H_2O solvent. None of the anions affected the fluorescence properties of probe Me-INDP in both PL and UV spectra. Moreover, when CN^- (10 μL) was added to the probe solution, an immediate color change was observed in the naked eye; the red color turned green under UV light. As Fig. 3 shows, the colorimetric and fluorescence responses of probe Me-INDP with various anions indicate that probe Me-INDP has a higher tendency to sense the cyanide anion selectively.

The sensing nature of Me-INDP towards CN^- was tested in the presence of other competitive species. Different species do not disturb the sensing nature of the Me-INDP towards CN^- anion (Fig. S5†).

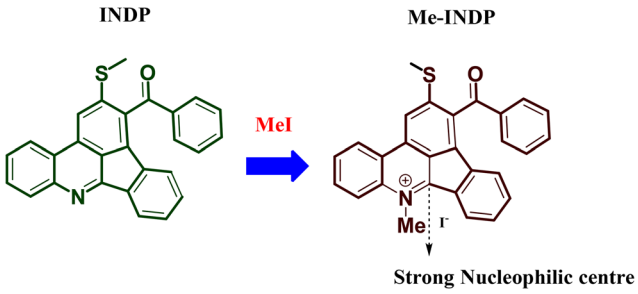

Scheme 1 Synthetic route for the probe Me-INDP.

The sensing mechanism of CN^-

The binding mechanism between Me-INDP and CN^- was investigated using Job's plot, ^{1}H NMR titration, ^{13}C NMR, SEM analysis, and DFT calculation. The Job's plot explored the stoichiometric binding ratio (1 : 1) between Me-INDP and CN^-. The NMR titration results agree with Job's plot and DFT calculation. With the increment of cyanide level, the NMR signal belonging to –NMe at δ 4.49 decreased to δ 4.34 (Fig. 4); this gradual upfield shows that the C_2 carbon is the binding site. The addition of CN^- on the C═N initiates the electron transfer from the carbon atom

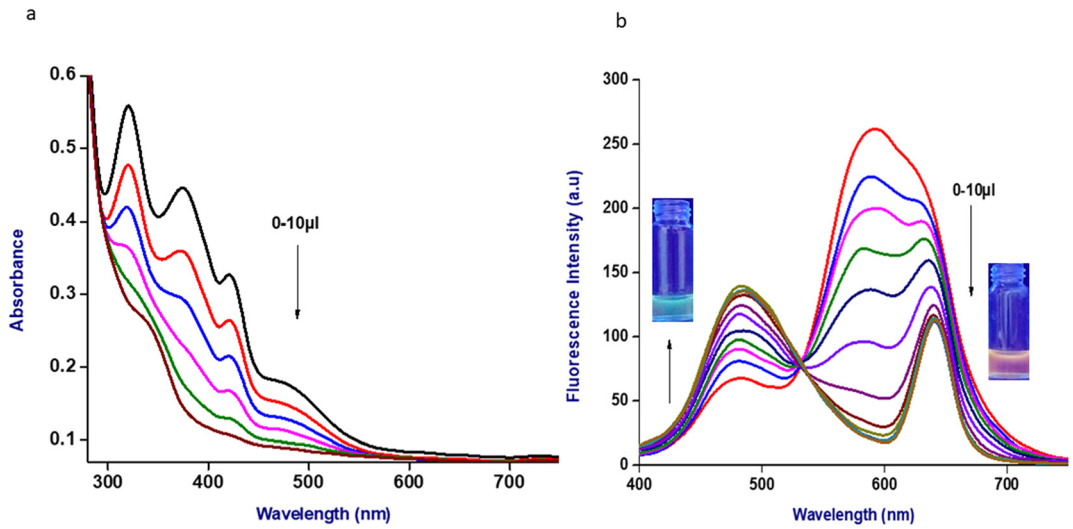

Fig. 1 (a) UV-vis spectra of probe Me-INDP with different concentrations of CN^- in ACN/H_2O (9 : 1). (b) Emission spectra of probe Me-INDP with different concentrations of CN^- in ACN/H_2O (9 : 1).

and neutralizes the positive charge on the nitrogen. The availability of electrons on the –NMe causes an upfield shift in ^1H NMR. Additionally, ^{13}C NMR titration was carried out to further confirm the proposed mechanism for the cyanide sensor by Me-INDP. In the carbon spectrum, C_1 and C_2 carbon peaks appeared at 39 and 140 ppm, respectively (Fig. 5). After the addition of nucleophilic CN, the C1 peak appeared at 34 ppm, and the C2 peak moved to 138 ppm. A new signal appeared at 118 ppm in the product corresponding to the C-atom for cyanide ions.

Recently, Elango *et al.* reported an ICT-based chemodosimeter for CN^- *via* nucleophilic addition on the C═N group (Scheme 2), and the reason behind the CN^- sensing mechanism of Me-INDP is shown in Scheme 3. The visible color and spectral changes were explained by the following factors: (i) the presence of a strong nucleophilic center on Me-INDP, which makes the irreversible addition on the C═N bond, after the addition of CN^-, (ii) the conversion of the quaternary ammonium complex to the pyridine scaffold, and (iii) loss of conjugation blocking the ICT for the phenanthridine unit.

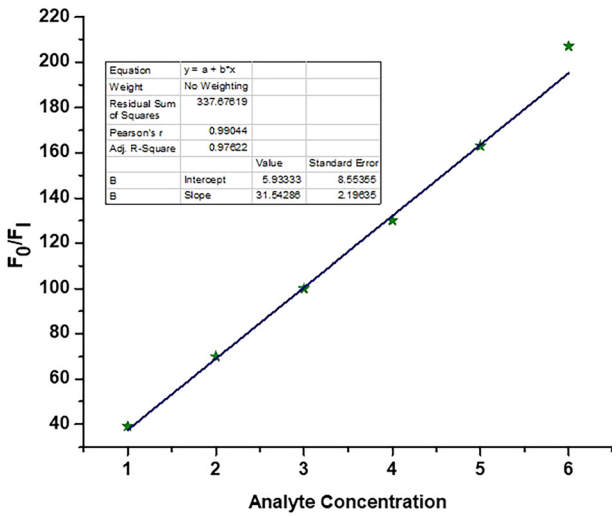

Fig. 2 Stern–Volmer plot.

Theoretical studies of the Me-INDP system

To gain insight into the mechanism of the probe with CN^-, theoretical study DFT calculation was performed in the Gaussian 05 program using B3LYP/3-21G basic level. In the HOMO of probe Me-INDP, the electron clouds over the phenanthridine unit. In LUMO, all the electron clouds move to the +N–Me group and its attached aromatic ring. This ICT creates the bright red fluorescence nature of Me-INDP. When the HOMO level of the probe is attached to the analyte Me-INDP–CN, the electron is localized on the whole molecule. In LUMO, all the electrons are transferred to the N–Me, CN group and its attached aromatic ring. After cyanide addition, the loss of π conjugation occured in Me-INDP, that prohibit the ICT mechanism, causes the emission vanished at visible region and obtained blue shift.

The energy gap between HOMO and LUMO of probe Me-INDP and adduct of Me-INDP–CN are 3.64 eV and 3.81 eV, respectively, as shown in Fig. 6. The calculated energy values of Me-INDP increased from 3.64 eV to 3.81 eV after nucleophilic reaction with CN^-. Increased energy values further confirmed the blue shift of the probe Me-INDP. The theoretical observation agrees with the experimental results from longer wavelengths to shorter wavelengths in the emission band.

Time responses of Me-INDP with CN^-

The rate of fluorescence changes in Me-INDP with cyanide was recorded at different time intervals. The wavelength of

Table 1 Comparison of the reported CN^- sensors with Me-INDP

Chemosensor	Limit of detection (LOD)	Binding constant	Solvent	References
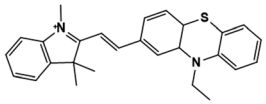	6.67 μM	$2.372 \times 10^4\ M^{-1}$	Tris HCL buffer	34
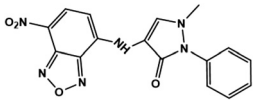	1.67 μM	$6.19 \times 10^6\ M^{-1}$	Aqueous methanol	35
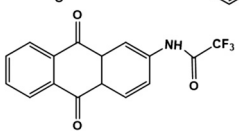	0.51 μM	$7.7 \times 10^4\ M^{-1}$	ACN/H_2O	36
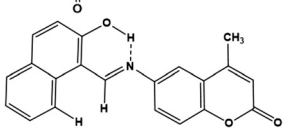	7.72 μM	$6.54 \times 10^4\ M^{-1}$	DMSO/H_2O	37
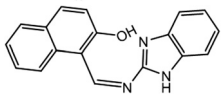	0.28 μM	$2.6 \times 10^3\ M^{-1}$	ACN/H_2O	38
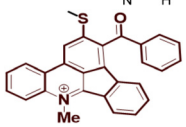	**1.2 nm**	**$3.1 \times 10^7\ M^{-1}$**	**ACN/H_2O**	**Present work**

Me-INDP at 580 nm and 480 nm reached constant intensity within one minute after CN^- addition. The PL changes were noted at different time intervals; no differences were obtained, and the PL intensity remained constant at different

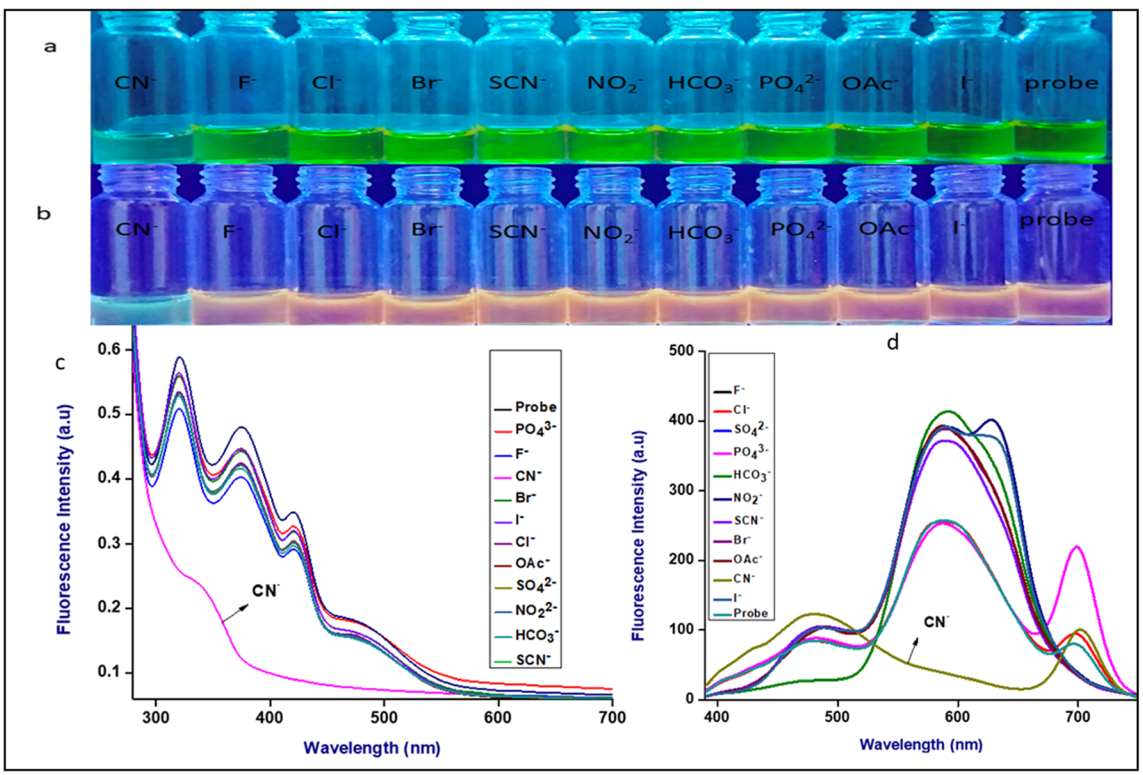

Fig. 3 (a) Naked eye color changes in probe Me-INDP with various anions. (b) Under a UV lamp, fluorescence changes in the probe with multiple anions. (c) UV-vis spectra of Me-IND (1×10^{-5} M) with different anions (10 μL). (d) Emission spectra of Me-IND (1×10^{-5} M) with various anions (10 μL).

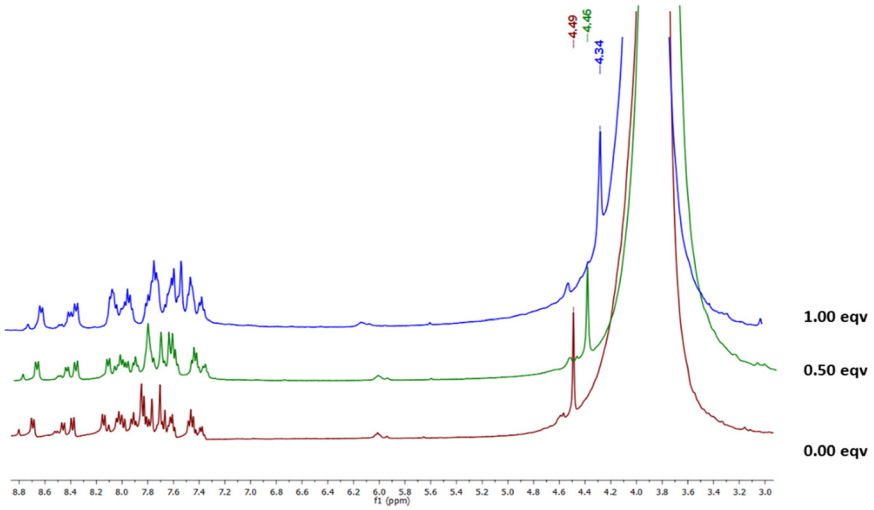

Fig. 4 NMR titration of probe Me-INDP with CN^- concentrations (in d_6-DMSO).

time scales in the range of 0–300 seconds, as shown in Fig. 7. Owing to the quick response and stability in time scale, the probe Me-INDP was suitable for the detection of cyanide ion in real-time applications.

SEM analysis

We performed SEM analysis to examine the aggregation morphology of the probe Me-INDP after addition with

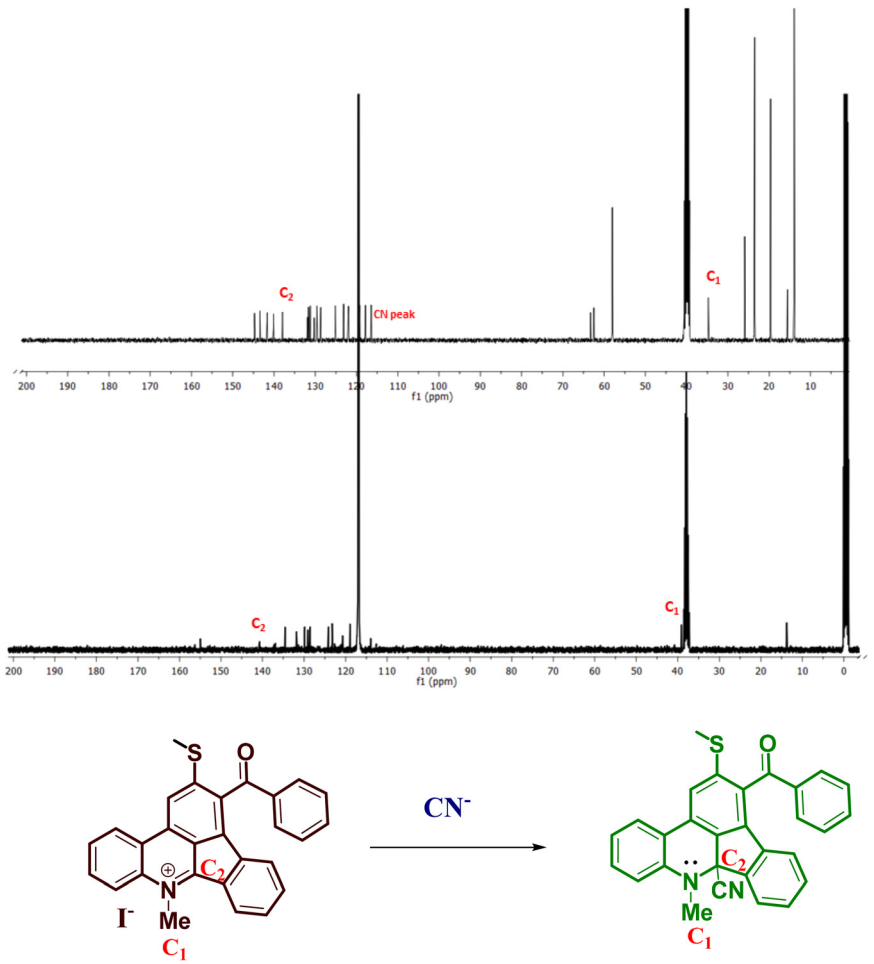

Fig. 5 ^{13}C NMR spectrum for reactant Me-INDP (bottom) and product after addition with CN^- (above) (in d_6-DMSO).

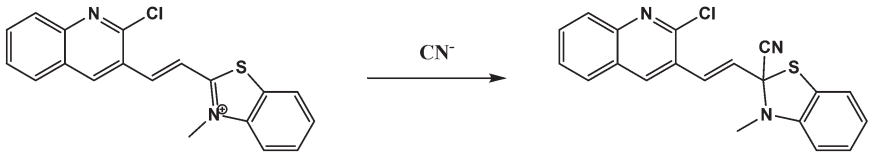

P. Elango *et al,* Anal. Methods, 2018, **10**, 2368–2375

Scheme 2 Ref. 33.

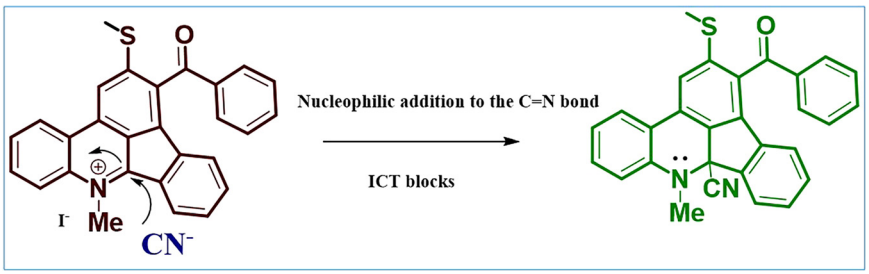

Scheme 3 Binding mechanism of Me-INDP with CN^-.

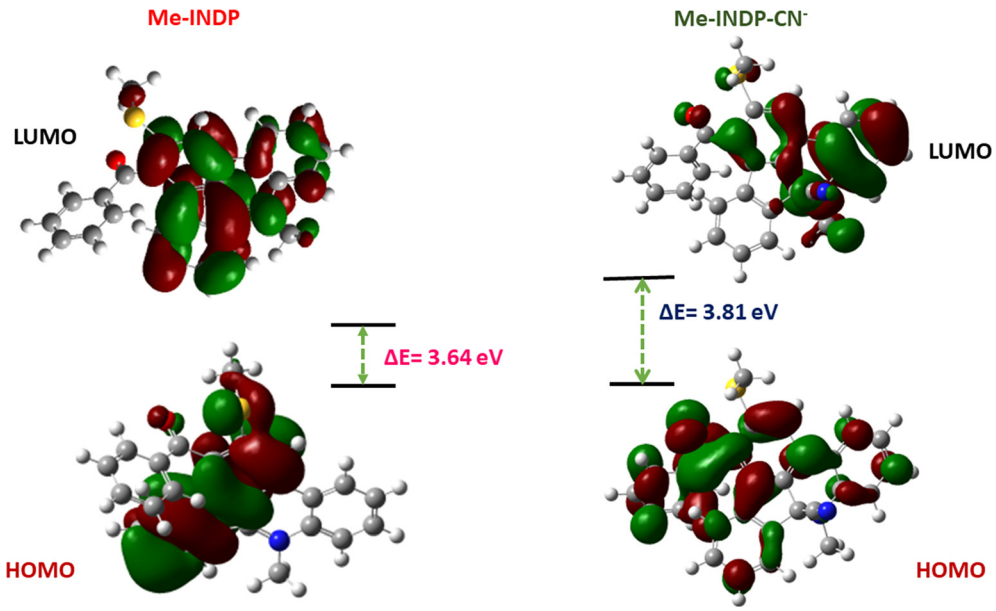

Fig. 6 Theoretical studies (DFT) of Me-INDP and Me-INDP–CN^- systems.

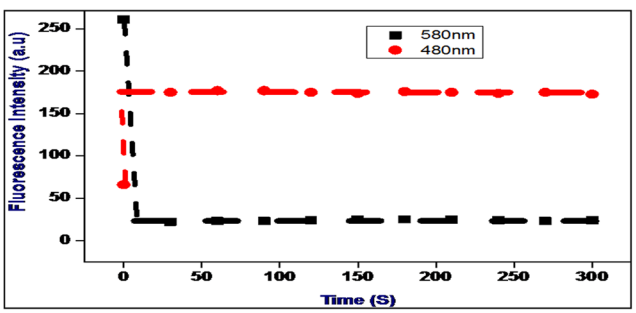

Fig. 7 Fluorescence intensity changes in 480 and 580 nm of Me-INDP treated after adding cyanide (10 μL) time-dependent.

cyanide concentration using the drop casting method. The morphology of Me-INDP (10^{-3} M) showed changes from granular deposition to the ordered dendritic shape after the addition of CN^- (10 μL) (Fig. 8). The obtained morphological change after the introduction of cyanide further supports the new fluorophore formation.

Real sample applications

The practical application of Me-INDP was used to detect the concentration of CN^- in natural water samples (river, sea) and cyanogenic food samples, such as almond, cassava flour, sprouted potatoes, and U87 cell lines.

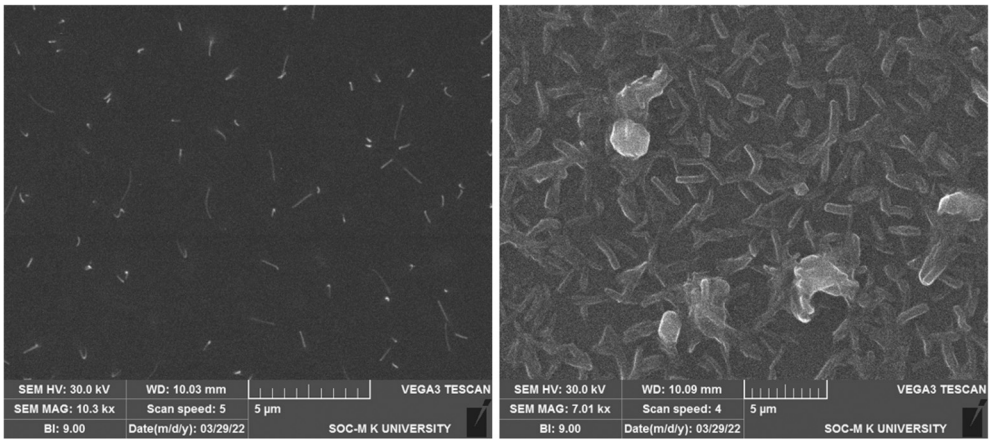

Fig. 8 SEM images of probe Me-INDP and probe with CN^- concentration.

Initially, the deduction of cyanide was checked in river and tap water; however, no detection was obtained. Afterward, the specific concentration of cyanide ion spiked in water samples.

Then, samples were used in the fluorometric experiment, with good recovery obtained for real samples (Fig. S7 and Table S1†). These results reveal that the probe Me-INDP has a high potential to predict cyanide in real samples. The food extracts were collected from commercially available almonds, cassava, and potatoes. Then, 10 μL of the section was added to the probe solution. Significant spectral changes were obtained when adding the food extracts to Me-INDP (Fig. 9).

Fluorescent bioimaging of Me-INDP and Me-INDP cyanide complex in U87 cell lines

The sensing behavior of Me-INDP for the detection of cyanide ion concentrations in a biological system was investigated using U87 cell lines. The probe Me-INDP in the cultivated cell lines without CN^- concentration emitted red fluorescence under a fluorescence microscope (Fig. 10). After adding 10 μL of CN^-, an immediate blueshift was obtained and emitted green fluorescence. These results suggested that the probe Me-INDP could efficiently detect the CN^- ions in a biological system.

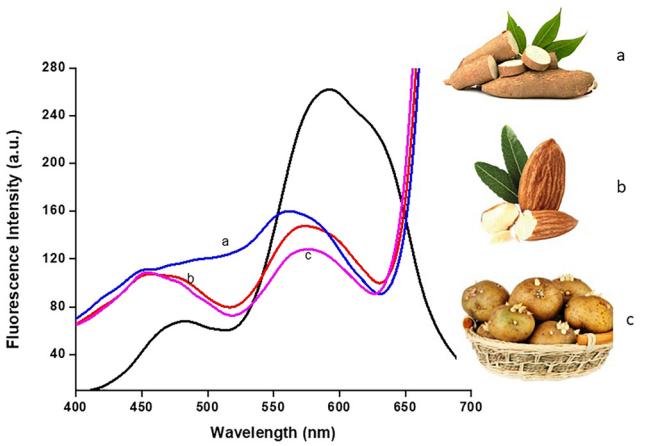

Fig. 9 Emission spectra of Me-INDP treated with food samples a) cassava flour, b) almonds, c) sprouted potatoes (10 μL) in ACN/H_2O (9 : 1).

Conclusion

In summary, we designed and synthesized the pyridinium-based chemosensor Me-INDP by a one-step reaction with good yield. Probe Me-INDP was selectively sensitive towards the concentration of CN^- in an ACN/H_2O medium with an excellent limit of detection of 1.2×10^{-9} M. The proposed mode of interaction between Me-INDP was revealed from the various experimental results involving absorption, fluorescence, job's plot, ^1H NMR, ^{13}C NMR, SEM analysis, and theoretical calculation. Sensor Me-INDP well potential utilization for sensing CN^- anions in food samples, accurate water analysis, and live-cell studies has a good relationship with experimental results.

Experimental section

The NMR spectra of the compounds were recorded on a Bruker (Advance) 400 MHz for ^1H and 100 MHz for ^{13}C using TMS as a standard internal DMSO-d_6 solvent. Chemical shifts are expressed in parts per million (ppm), and the coupling constants (J values) are described in hertz (Hz). The photoluminescence and absorption spectra were recorded by employing a Spectramax m2e spectrophotometer. The sample was placed in a 1 mL quartz cuvette to obtain both PL and absorption spectra. HR-Mass data were recorded on Agilent Accurate-Mass Q-TOF (model HAB 273). All chemicals were purchased from Sigma-Aldrich without any further purification. A mixture of pet ether and ethyl acetate (9 : 1 ratio) was used as an eluent.

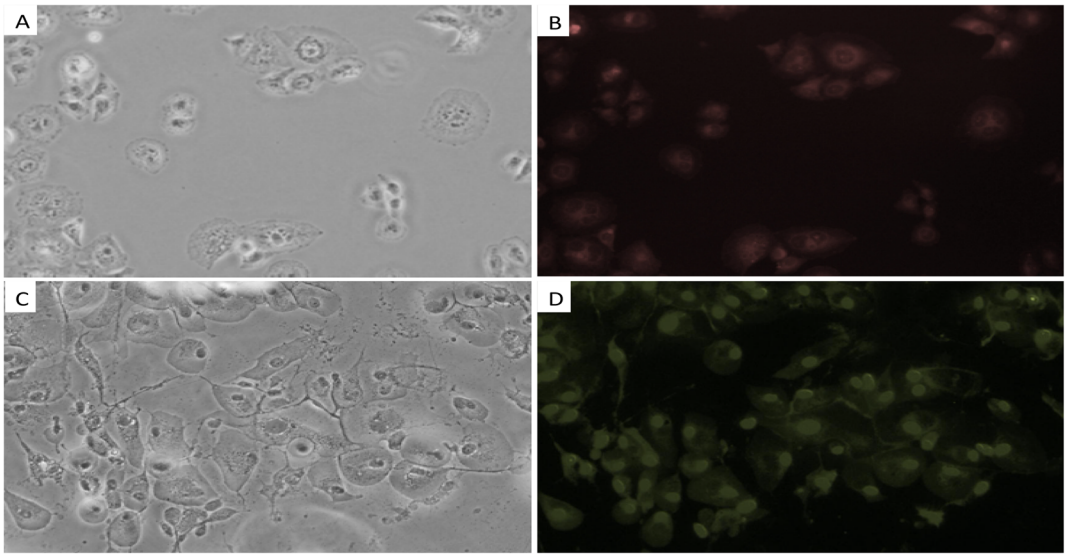

Fig. 10 Investigation of cyanide sensing in U87 cell lines. (A) Bright field images of probe-treated cells, (B) fluorescent images of probe-treated cells, (C) bright-field images of probe treated with cyanide, and (D) fluorescent images of probe treated with cyanide.

UV-vis and photoluminescence experiments

The stock solution of Me-INDP was prepared with 1×10^{-3} M concentration in ACN solvent. The CN^- stock solution was prepared in 1×10^{-2} M concentration using tetrabutylammonium cyanide in double distilled water. All the other anion solutions were designed using DD water from respective salts. The PL studies were carried out for probe Me-INDP when the excitation wavelength was 320 nm under normal room temperature.

Detection of cyanide ion in real water samples

Real water samples were collected from the Thamirabarani river, and tab water 1 and tab water 2 were collected from around Madurai city areas. The detection of cyanide concentration was carried out with 1 mL of real water added with 10 μL probe solution from bulk concentration; the amount of spiked volume of cyanide is 10 μL from the bulk solution.

Detection of cyanide ion in food samples

The cassava flour, almonds, and sprouted potatoes were collected from the commercially available market. The food extracts were separated from 5 g of each food sample that was finely crushed with 5 mL of DD water, and 0.05 g NaOH was added and centrifuged at 1000 rpm for 20 min. After that, clear food extracts were collected and used for the experiment.

Detection of cyanide in biological samples

U87 cells were treated with an assigned IC_{50} probe concentration to visualize the fluorescent properties. Initially, 0.3×10^6 of U87 cells were seeded in 6 well plates and incubated up to 80% confluency. Later, cyanide sensing in the cell lines was analyzed by treating the U87 cells with a probe for an hour, followed by the addition of cyanide at a 1 : 10 ratio. The changes in the luminescence were visualized under a fluorescent microscope. The cells treated with only the probe Me-INDP served as a standard control for the comparative screening of the probe Me-INDP–cyanide complex.

A general method for the synthesis of probe INDP

A mixture of OKDTA 1 (1.0 mmol) and indenoquinoline 5 (1.0 mmol) was treated in base sodium *tert*-butoxide under ice-cold conditions. After 10 minutes, it was allowed to be stirred at room temperature for 3–4 h (appropriate time). The completion of the reaction was monitored by applying the TLC method. After the reaction was completed, the reaction mixture was treated with 10% HCl solution and stirred for 10–15 minutes. A yellow precipitate was formed and collected by filtration. The crude residue was recrystallized to obtain a pure solid product of INDP, as previously described in our previous study.

A general method for the synthesis of the probe Me-INDP

The synthesized compound INDP (1.0 mmol) was well dissolved in DCM. After that, methyl iodide (MEI) (5.0 mmol) was added to the reaction solution in the dropwise addition method under cold conditions 0 °C. The reaction mixture was allowed to stir up for 12 hours. Subsequently, a red precipitate was formed. TLC monitored the completion of the reaction. The red precipitate was collected by employing the filtration method, and the residue was not required for further purification.

(2-(Methyltphenanthridine2,3-*gh*)phenanthridin-1-*yl*)(phenyl)methanone (INDP). Yield: 92%. Yellow solid, mp 199–200 °C.^{1}H NMR (400 MHz, $CDCl_3$): δ 2.73 (s, 3H, –SMe),

7.26 (s, 2H), 7.41–7.54 (m, 3H), 7.66–7.73 (m, ddd, J = 29.1, 15.4, 7.3 Hz, 5H), 8.01 (s, 1H), 8.20 (d, J = 7.0 Hz, 1H), 8.32 (d, J = 8.2 Hz, 1H), 8.47 (d, J = 7.9 Hz, 1H), ^{13}C NMR (100 MHz, $CDCl_3$): δ 15.9, 109.6, 116.8, 118.1, 121.8, 122.8, 123.3, 126.8, 127.5, 127.6, 128.4, 128.8, 129.7, 130.5, 131.7, 138.0, 141.3, 145.2, 147.9, 160.6. IR spectrum (cm^{-1}): 2969.64, 1701.90 (C═O), 1436.97, 1086.26, 961.17, 755.69, 645.45. HRMS (ES-MS TOF) m/z: $[M–H]^+$ calcd for $C_{27}H_{17}NOS$ 403.1031: found fragmentation peak $[M + H]^+$ calcd for $C_{20}H_{13}NS$ at 300.0840.

1-Benzoyl-8-methyl-2-(methylthio)indeno[1,2,3-*gh*] phenanthridin-8-ium (Me-INDP). Isolated yield: 85%, red solid, mp: 200 °C ^{1}H NMR (400 MHz, DMSO) δ 8.69 (d, J = 8.1 Hz, 1H), 8.39 (d, J = 8.8 Hz, 1H), 8.18 (d, J = 7.9 Hz, 1H), 8.10–8.03 (m, 1H), 7.96 (t, J = 7.6 Hz, 1H), 7.84–7.76 (m, 1H), 7.66 (dd, J = 17.8, 10.3 Hz, 1H), 7.54–7.39 (m, 1H), 4.58 (s, 1H), 2.67 (s, 1H). ^{13}C NMR (100 MHz, DMSO) δ 156.26 (s), 154.94 (s), 140.74 (s), 137.20 (s), 136.85 (s), 134.56 (s), 131.84 (s), 129.83 (s), 129.05 (s), 128.57 (s), 124.15 (s), 123.23 (s), 122.67 (s), 121.14 (s), 120.72 (s), 118.92 (s), 113.95 (s), 112.59 (s), 39.15 (s), 13.75 (s). IR spectrum (cm^{-1}): 2994.81, 1716.26 (C═O), 1622.04, 1417.91, 1082.35, 754.01, 655.62. HRMS (ES-MS TOF) m/z: $[M–H]^+$ calcd for $C_{28}H_{20}NOS^+$ 418.16: found [M + Na] adduct calcd for $[C_{28}H_{20}NOSNa]$ at 441.2989.

Conflicts of interest

The authors declared no conflicts of interest.

Acknowledgements

SS thanks to SERB-CRG (EMR)–MRP New Delhi, India, for financial assistance. JK, thank SERB for the fellowship. Also, we thank DST-FIST/PURSE, RUSA and TANSCHE for the joint funding and instruments facility.

References

1 Z. Zhang, Z. Wu, J. Sun, B. Yao, G. Zhang, P. Xue and R. Lu, Mechanofluorochromic properties of β-iminoenolate boron complexes tuned by the electronic effects of terminal phenothiazine and phenothiazine-S, S-dioxide, *J. Mater. Chem. C*, 2015, **3**, 4921–4932.

2 C. Dou, L. Han, S. Zhao, H. Zhang and Y. Wang, Multi-stimuli-responsive fluorescence switching of a donor-acceptor π-conjugated compound, *J. Phys. Chem. Lett.*, 2011, **2**, 666–670.

3 U. Balijapalli, S. Udayadasan, E. Shanmugam and S. K. Iyer, Synthesis, photophysical, and acid chromic properties of a series of tetrahydrodibenzo [a, i] phenanthridine chromophores, *Dyes Pigm.*, 2016, **130**, 233–244.

4 P. Meti and Y. D. Gong, Unveiling the photophysical and morphological properties of an acidochromic thiophene flanked dipyrrolopyrazine-based chromophore for optoelectronic application, *RSC Adv.*, 2018, **8**, 2004–2014.

5 F. Rafiee, Synthesis of phenanthridine and phenanthridine derivatives based on Pd-catalyzed C–H activation, *Appl. Organomet. Chem.*, 2017, **31**, 3820.

6 L. Long, X. Yuan, S. Cao, Y. Han, W. Liu, Q. Chen, Z. Han and K. Wang, Determination of cyanide in water and food samples using an efficient naphthalene-based ratiometric fluorescent probe, *ACS Omega*, 2019, **4**, 10784–10790.

7 A. K. Nath, X. Shi, D. L. Harrison, J. E. Morningstar, S. Mahon, A. Chan, P. Sips, J. Lee, C. A. MacRae, G. R. Boss and M. Brenner, Cisplatin analogs confer protection against cyanide poisoning, *Cell Chem. Biol.*, 2017, **24**, 565–575.

8 M. K. Bera, C. Chakraborty, P. K. Singh, C. Sahu, K. Sen, S. Maji, A. K. Das and S. Malik, Fluorene-based chemodosimeter for "turn-on" sensing of cyanide by hampering ESIPT and live cell imaging, *J. Mater. Chem. B*, 2014, **2**, 4733–4739.

9 M. La, Y. Hao, Z. Wang, G. C. Han and L. Qu, Selective and sensitive detection of cyanide based on the displacement strategy using a water-soluble fluorescent probe, *J. Anal. Methods Chem.*, 2016, **2016**, 1462013.

10 Z. Li, C. Rao, L. Chen, C. Fu, T. Zhu, X. Chen and C. Liu, Addition of α-cyanomethylpyridine to naphthalimide via trifluoromethyl-directed CH functionalization: cyanide sensing in aqueous media, *J. Org. Chem.*, 2019, **84**, 7518–7522.

11 (*a*) T. Zhu, Z. Li, C. Fu, L. Chen, X. Chen, C. Gao, S. Zhang and C. Liu, Development of an anthraquinone-based cyanide colorimetric sensor with activated C–H group: large absorption redshift and application in food and water samples, *Tetrahedron*, 2020, **76**, 131479; (*b*) F. Zelder and L. Tivana, Corrin-based chemosensors for the assured detection of endogenous cyanide, *Org. Biomol. Chem.*, 2015, **13**, 14–17.

12 C. Baird and M. Cann, *Environmental Chemistry*, WH, New York, 2005, p. 608.

13 H. H. Yang, P. P. Liu, J. P. Hu, H. Fang, Q. Lin, Y. Hong, Y. M. Zhang, W. J. Qu and T. B. Wei, A fluorescent supramolecular gel and its application in the ultrasensitive detection of CN^- by anion–π interactions, *Soft Matter*, 2020, **16**, 9876–9881.

14 S. Chakraborty, S. Paul, P. Roy and S. Rayalu, Detection of Cyanide ion by Chemosensing and Fluorosensing Technology, *Inorg. Chem. Commun.*, 2021, 108562.

15 S. Naha, S. P. Wu and S. Velmathi, Naphthalimide based smart sensor for CN^-/Fe^{3+} and H_2S. Synthesis and application in RAW264. 7 cells and zebrafish imaging, *RSC Adv.*, 2020, **10**, 8751–8759.

16 Y. Yue, F. Huo, C. Yin, J. Chao and Y. Zhang, A new "donor-two-acceptor" red emission fluorescent probe for highly selective and sensitive detection of cyanide in living cells, *Sens. Actuators, B*, 2015, **212**, 451–456.

17 L. Long, Y. Han, X. Yuan, S. Cao, W. Liu, Q. Chen, K. Wang and Z. Han, A novel ratiometric near-infrared fluorescent probe for monitoring cyanide in food samples, *Food Chem.*, 2020, **331**, 127359.

18 R. Koenig, Wildlife deaths are a grim wake-up call in Eastern Europe, *Science*, 2000, **287**, 1737–1738.

19 A. Alizadeh, S. Ghouzivand, M. M. Khodaei and M. Ardalani, An interesting spectroscopic method for chromofluorogenic

detection of cyanide ion in aqueous solution: Disruption of intramolecular charge transfer (ICT), *J. Chem. Sci.*, 2016, **128**, 537–543.

20 W. J. Qu, W. T. Li, H. L. Zhang, T. B. Wei, Q. Lin, H. Yao and Y. M. Zhang, Rapid and Selective Detection of Cyanide Anion by Enhanced Fluorescent Emission and Colorimetric Color Change at Micromole Levels in Aqueous Medium, *J. Heterocyclic Chem.*, 2018, **55**, 879–887.

21 Z. Liu, X. Wang, Z. Yang and W. He, Rational design of a dual chemosensor for cyanide anion sensing based on dicyanovinyl-substituted benzofuran, *J. Org. Chem.*, 2011, **76**, 10286–10290.

22 H. Nzwalo and J. Cliff, Konzo: from poverty, cassava, and cyanogen intake to toxico-nutritional neurological disease, *PLoS Neglected Trop. Dis.*, 2011, **5**, 1051.

23 Z. Xu, X. Chen, H. N. Kim and J. Yoon, Sensors for the optical detection of cyanide ion, *Chem. Soc. Rev.*, 2010, **39**, 127–137.

24 X. X. Ou, Y. L. Jin, X. Q. Chen, C. B. Gong, X. B. Ma, Y. S. Wang and Q. Tang, Colorimetric test paper for cyanide ion determination in real-time, *Anal. Methods*, 2015, **7**, 5239–5244.

25 J. L. Sessler and D. G. Cho, The benzil rearrangement reaction: trapping of a hitherto minor product and its application to the development of a selective cyanide anion indicator, *Org. Lett.*, 2008, **10**, 73–75.

26 Y. Sun, G. Wang and W. Guo, Colorimetric detection of cyanide with N-nitrophenyl benzamide derivatives, *Tetrahedron*, 2009, **65**, 3480–3485.

27 Y. Kim, H. Zhao and F. P. Gabbaï, Sulfonium boranes for the selective capture of cyanide ions in water, *Angew. Chem., Int. Ed.*, 2009, **48**, 4957–4960.

28 P. B. Pati, Organic chemodosimeter for cyanide: A nucleophilic approach, *Sens. Actuators, B*, 2016, **222**, 374–390.

29 Y.-K. Yang and J. Tae, Acridinium salt based fluorescent and colorimetric chemosensor for the detection of cyanide in water, *Org. Lett.*, 2006, **8**, 5721–5723.

30 (*a*) J. L. Sessler and D. G. Cho, The benzil rearrangement reaction: trapping of a hitherto minor product and its application to the development of a selective cyanide anion indicator, *Org. Lett.*, 2008, **10**, 73–75; (*b*) S. Chakraborty, S. Paul, P. Roy and S. Rayalu, Detection of cyanide ion by chemosensing and fluorosensing technology, *Inorg. Chem. Commun.*, 2021, **128**, 108562.

31 E. Thanayupong, K. Suttisintong, M. Sukwattanasinitt and N. Niamnont, Turn-on fluorescent sensor for the detection of cyanide based on a novel dicyanovinyl phenylacetylene, *New J. Chem.*, 2017, **41**, 4058–4064.

32 S. Shanmugam, K. Jamuna, T. Solaimalai, A. M. Kubendran and A. Balasubramaniem, Synthesis of Indenophenanthridine via [4+ 2] Annulation Strategy: "Turn-Off" Fe^{3+} Ion Sensor, Practical Application in Live Cell Imaging and Reversible Acidochromism Studies, *New J. Chem.*, 2022, **46**, 9207–9213.

33 (*a*) P. R. Lakshmi, R. Manivannan, P. Jayasudha and K. P. Elango, An ICT-based chemodosimeter for selective dual channel sensing of cyanide in an aqueous solution, *Anal. Methods*, 2018, **10**, 2368–2375; (*b*) T. F. Robbins, H. Qian, X. Su, R. P. Hughes and I. Aprahamian, Cyanide detection using a triazolopyridinium salt, *Org. Lett.*, 2013, **15**, 2386–2389.

34 J. V. Ros-Lis, R. Martínez-Manez and J. Soto, A selective chromogenic reagent for cyanide determination, *Chem. Commun.*, 2002, 2248–2249.

35 (*a*) T. Zhu, Z. Li, C. Fu, L. Chen, X. Chen, C. Gao and C. Liu, Development of an anthraquinone-based cyanide colorimetric sensor with activated C–H group: large absorption redshift and application in food and water samples, *Tetrahedron*, 2020, **76**, 131479; (*b*) Y. L. Leng, J. H. Zhang, Q. Li, Y. M. Zhang, Q. Lin, H. Yao and T. B. Wei, A highly sensitive colorimetric chemodosimeter for cyanide anion by Michael addition based on a coumarin derivative, *New J. Chem.*, 2016, **40**, 8607–8613.

36 M. Sun, S. Wang, Q. Yang, X. Fei, Y. Li and Y. Li, A new colorimetric fluorescent sensor for ratiometric detection of cyanide in solution, test strips, and in cells, *RSC Adv.*, 2014, **4**, 8295–8299.

37 T. Anand and M. Sankar, A dual colorimetric chemosensor for Hg (ii) and cyanide ions in aqueous media based on a nitrobenzoxadiazole (NBD)–antipyrine conjugate with INHIBIT logic gate behaviour, *Anal. Methods*, 2020, **12**, 4526–4533.

38 H. T. Niu, D. Su, X. Jiang, W. Yang, Z. Yin, J. He and J. P. Cheng, A simple yet highly selective colorimetric sensor for cyanide anion in an aqueous environment, *Org. Biomol. Chem.*, 2008, **6**, 3038–3040.